

# Sphingosine derivatives inhibit cell signaling by electrostatically neutralizing polyphosphoinositides at the plasma membrane

Norah L. Smith, Stephanie Hammond, Deepti Gadi, Alice Wagenknecht-Wiesner, Barbara Baird and David Holowka\*

Department of Chemistry and Chemical Biology; Cornell University; Ithaca, NY USA

**Key words:** IgE receptors, cholera toxin B, recycling endosomes,  $\text{Ca}^{2+}$  signaling,  $\text{PIP}_2$

Mast cell stimulation via IgE receptors causes activation of multiple processes, including  $\text{Ca}^{2+}$  mobilization, granule exocytosis, and outward trafficking of recycling endosomes to the plasma membrane. We used fluorescein-conjugated cholera toxin B (FITC-CTxB) to label  $\text{GM}_1$  in recycling endosomes and to monitor antigen-stimulated trafficking to the plasma membrane in both fluorimeter and imaging-based assays. We find that the sphingosine derivatives D-sphingosine and N,N'-dimethylsphingosine effectively inhibit this outward trafficking response, whereas a quarternary ammonium derivative, N,N',N''-trimethylsphingosine, does not inhibit. This pattern of inhibition is also found for  $\text{Ca}^{2+}$  mobilization and secretory lysosomal exocytosis, indicating a general effect on  $\text{Ca}^{2+}$ -dependent signaling processes. This inhibition correlates with the capacity of sphingosine derivatives to flip to the inner leaflet of the plasma membrane that is manifested as changes in plasma membrane-associated FITC-CTxB fluorescence and cytoplasmic pH. Using a fluorescently labeled MARCKS effector domain to monitor plasma membrane-associated polyphosphoinositides, we find that these sphingosine derivatives displace the electrostatic binding of this MARCKS effector domain to the plasma membrane in parallel with their capacity to inhibit  $\text{Ca}^{2+}$ -dependent signaling. Our results support roles for plasma membrane polyphosphoinositides in  $\text{Ca}^{2+}$  signaling and stimulated exocytosis, and they illuminate a mechanism by which D-sphingosine regulates signaling responses in mammalian cells.

*Do not distribute.*

## Introduction

Mast cells play important roles in inflammation and allergic disease. In response to antigen-mediated crosslinking, IgE receptors, FcεRI, initiate a complex signaling cascade that results in exocytosis of secretory lysosomes and stimulated production of numerous cytokines in these cells.<sup>1</sup> Previously, our laboratory developed a fluorescence assay for trafficking of recycling endosomes in RBL mast cells that monitors pH-dependent changes in the fluorescence of FITC-CTxB and FITC-anti-transferrin receptor mAb, and we showed that antigen stimulates increased recycling endosomal trafficking to the plasma membrane.<sup>2</sup> This trafficking response was found to be largely insensitive to inhibitors of downstream enzymes in secretory lysosomal exocytosis, including PI3-kinase and protein kinase C, but was reduced by the absence of extracellular  $\text{Ca}^{2+}$  and by U73122, an inhibitor of inositol 1,4,5-triphosphate production leading to  $\text{Ca}^{2+}$  mobilization.<sup>3</sup>

Recycling endosomes were first identified as a perinuclear pool of tubular and vesicular membranes containing transferrin receptors.<sup>4</sup> This membrane pool is mildly acidic and is distinct from the early and sorting endosomes as well as from the Golgi complex.<sup>5</sup> It has been shown to participate in regulating the

directionality of epithelial cell migration<sup>6</sup> and the maintenance of cell polarity,<sup>7,8</sup> as well as in phagocytosis<sup>9</sup> and cytokinesis.<sup>10</sup> Furthermore, there is evidence that recycling endosomes play roles in various diseases, including enhancement of HIV viral particle release<sup>11</sup> and influence neuro-degenerative diseases such as Alzheimer's disease.<sup>12</sup> Studies have also provided evidence for their role in stimulated secretion of cytokines in hematopoietic cells.<sup>13</sup>

In the course of investigating selective inhibition of stimulated recycling endosome trafficking to the plasma membrane, we found that certain sphingosine derivatives are particularly effective inhibitors of this process in RBL mast cells. This inhibition correlates with inhibition of stimulated  $\text{Ca}^{2+}$  mobilization that is important for exocytosis of recycling endosomes as well as secretory lysosomes. Furthermore, this inhibition depends on the capacity of sphingosine bases to flip to the inner leaflet of the plasma membrane and to mediate electrostatic neutralization of polyphosphoinositides at this cytoplasmic interface. These results confirm an important role for  $\text{Ca}^{2+}$  signaling in stimulation of recycling endosomal trafficking, and they provide new insights into the mechanism by which both exogenous and endogenous sphingosines can regulate stimulated signaling in eukaryotic cells.

\*Correspondence to: David Holowka; Email: dah24@cornell.edu

Submitted: 01/18/10; Revised: 03/02/10; Accepted: 03/03/10

Previously published online: [www.landesbioscience.com/journals/selfnonself/article/11672](http://www.landesbioscience.com/journals/selfnonself/article/11672)

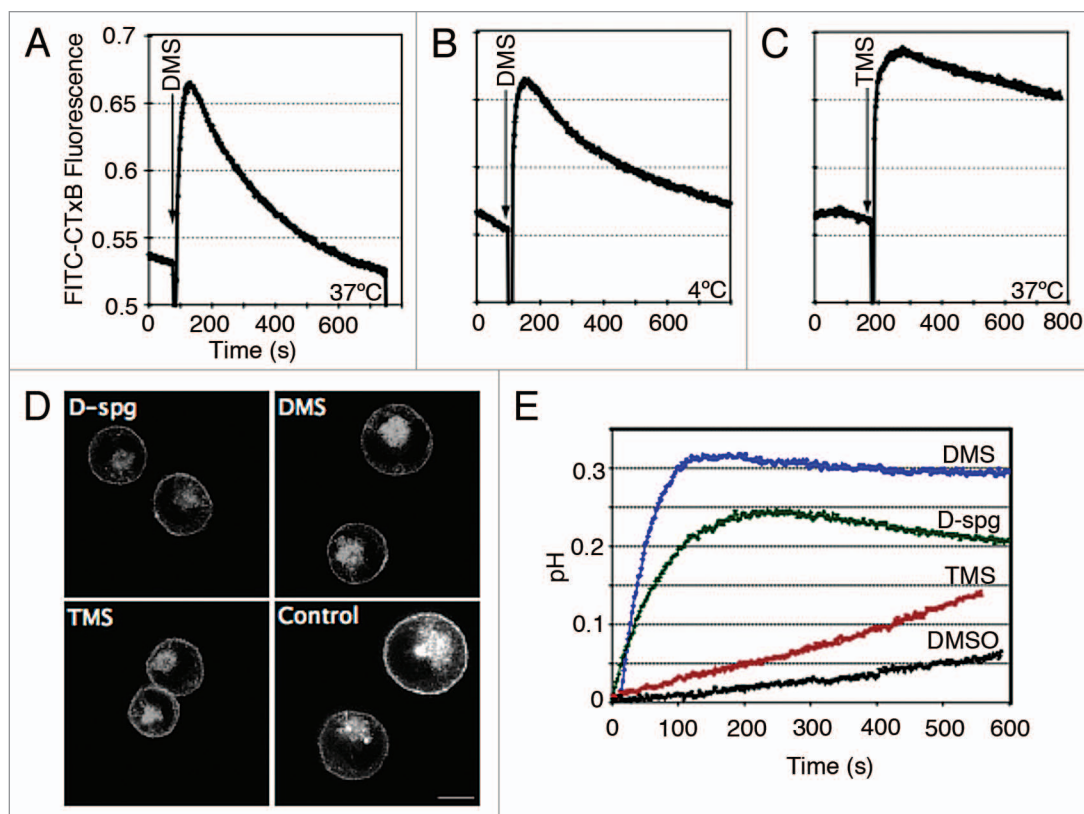


**Figure 1.** Sphingosine derivatives cause transient increases in the fluorescence of FITC-CTxB bound to GM<sub>1</sub> that correlates with cytoplasmic alkalinization. (A–C) RBL-2H3 cells were labeled with FITC-CTxB 37°C or 4°C, and 8  $\mu$ M DMS or TMS were added as indicated. (D) Confocal equatorial images of RBL-2H3 cells labeled with Alexa488-CTxB for 2 hr at 37°C, then treated with 8  $\mu$ M D-sphingosine (D-spg), DMS or TMS for 10 min prior to fixation and imaging. Scale bar = 10  $\mu$ m. (E) Changes in BCECF fluorescence in labeled RBL-2H3 cells in response to sphingosine derivatives (8  $\mu$ M) or solvent (0.05% v/v DMSO) alone. Data in (A–E) are representative of at least three independent experiments.

## Results

**Sphingosine derivatives cause transient increases in surface FITC-CTxB fluorescence that correlates with insertion and flipping in the plasma membrane.** In our previous study of recycling endosome trafficking, we determined that Ca<sup>2+</sup> influx is necessary for sustained outward trafficking of recycling endosomes in RBL mast cells.<sup>2</sup> Ca<sup>2+</sup> mobilization during IgE-Fc $\epsilon$ RI-mediated signaling involves both release of Ca<sup>2+</sup> from stores and influx via the store-operated Ca<sup>2+</sup> entry (SOCE) channel Orai1/CRACM1.<sup>22,23</sup> It was shown previously that sphingosine derivatives effectively block SOCE,<sup>24</sup> so we examined the effects of several sphingosine derivatives on outward trafficking of FITC-CTxB in RBL cells.

In initial experiments, we found that addition of 8  $\mu$ M D-sphingosine or N,N'-dimethylsphingosine (DMS) to cells labeled with FITC-CTxB at 37°C caused a rapid increase in FITC fluorescence that decayed back to its original intensity after ~10 min (Fig. 1A and data not shown). To determine whether this response is due to stimulated outward trafficking of CTxB from recycling endosomes, cells were labeled at 4°C to confine labeling to the plasma membrane.<sup>2</sup> Under these conditions, a similar transient increase in FITC fluorescence was observed upon addition of these derivatives, with no detectable

change in the cellular distribution of label (Fig. 1B and data not shown), indicating that this reflects a change in plasma membrane-associated FITC fluorescence. By comparison, addition of N,N',N''-trimethylsphingosine (TMS), the quaternary ammonium derivative, to cells labeled with FITC-CTxB at 37°C causes a similar rapid increase in FITC-CTxB fluorescence, but this higher level of fluorescence is more sustained over the same timescale (Fig. 1C). Under these conditions, none of these sphingosine derivatives cause visible changes in the distributions of FITC-CTxB or Alexa488-CTxB (Fig. 1D) at the plasma membrane and the recycling endosomal pool.

In other experiments, we found that cells labeled with pH-insensitive Alexa488-CTxB showed a similar, transient increase fluorescence in response to DMS, suggesting that it represents transient relief of self-quenching of the CTxB conjugates at the cell surface, rather than a pH-dependent effect on FITC fluorescence (data not shown). Furthermore, these sphingosine derivatives do not alter the fluorescence of CTxB conjugates in solution or that of FITC-IgE bound to Fc $\epsilon$ RI at the cell surface (data not shown), indicating an effect that depends on the specific protein ligand (CTxB) bound to GM<sub>1</sub> at the cell surface.

These results suggest that the increase in fluorescence observed is due to the insertion of the sphingosine compounds into the outer leaflet of the plasma membrane, which relieves FITC-CTxB

self-quenching at the cell surface. D-sphingosine and DMS in Triton X-100 micelles and lipid bilayers have pKa values of 8.5,<sup>25</sup> and 8.8,<sup>26</sup> respectively, and thus exist largely as protonated, positively charged species at pH 7.2, whereas the quarternary amine derivative TMS is positively charged at all pH values. Because of this charge, the latter derivative has a very low probability of flipping to the inner leaflet of the plasma membrane at any time,<sup>27</sup> whereas this probability is significant for DMS and D-sphingosine, which both undergo deprotonation at a small but finite probability at pH 7.2. Thus, the biphasic nature of the FITC-CTxB fluorescence change induced by DMS and D-sphingosine is likely due to their insertion, then time-dependent flipping to the inner leaflet of the plasma membrane. In this process, the uncharged sphingosine species would regain a proton at the inner leaflet as dictated by its pKa and the cytoplasmic pH (~7.4).

To test this hypothesis, we loaded RBL-2H3 cells in suspension with cell permeable BCECF-AM, a fluorescein-based pH sensor,<sup>18</sup> and monitored BCECF fluorescence during addition of sphingosine derivatives. As shown in Figure 1E, 8  $\mu$ M D-sphingosine and DMS both caused a time-dependent increase in the cytoplasmic pH by 0.2–0.3 pH units that becomes maximal after 100–200 sec. By comparison, the same concentration of TMS caused a much slower increase in BCECF fluorescence that was only a little larger than the baseline change in the presence of solvent alone. These results indicate that the transient increase in FITC-CTxB fluorescence caused by D-sphingosine and DMS can be accounted for by their insertion into the plasma membrane, followed by their flipping to its inner leaflet upon deprotonation, where they become reprotonated and thereby increase the cytoplasmic pH. For TMS, the slow decline of FITC-CTxB fluorescence following its rapid increase, and the slow, small increase in BCECF fluorescence following addition of TMS that are observed (Fig. 1C and E) may be due to impurities in this preparation, such as small amounts of DMS.

**D-sphingosine and DMS inhibit outward trafficking of FITC-CTxB-labeled recycling endosomes.** As previously described, antigen stimulates a rapid increase in FITC fluorescence from RBL cells that are sensitized with IgE and labeled with FITC-CTxB at 37°C (Fig. 2A, left), and this was shown to reflect stimulated outward trafficking of labeled recycling endosomes.<sup>2</sup> As illustrated in Figure 2A, right, addition of the inhibitor of actin polymerization, cytochalasin D, prior to stimulation enhances the magnitude and duration of the stimulated trafficking response.<sup>2</sup> Because cytochalasin D provides a stronger, more sustained response to antigen, we carried out subsequent trafficking experiments under these conditions. To evaluate the effects of sphingosine derivatives on stimulated trafficking of FITC-CTxB-labeled recycling endosomes, RBL cells sensitized with IgE and labeled with FITC-CTxB at 37°C were treated with different sphingosine derivatives for 10 min prior to addition of cytochalasin D and antigen. The fluorescence baseline was monitored for several minutes subsequent to addition of cytochalasin D, and this was extrapolated and subtracted as described in Materials and Methods.

As shown in Figure 2B, both D-sphingosine and DMS substantially reduce the trafficking response to antigen, with some

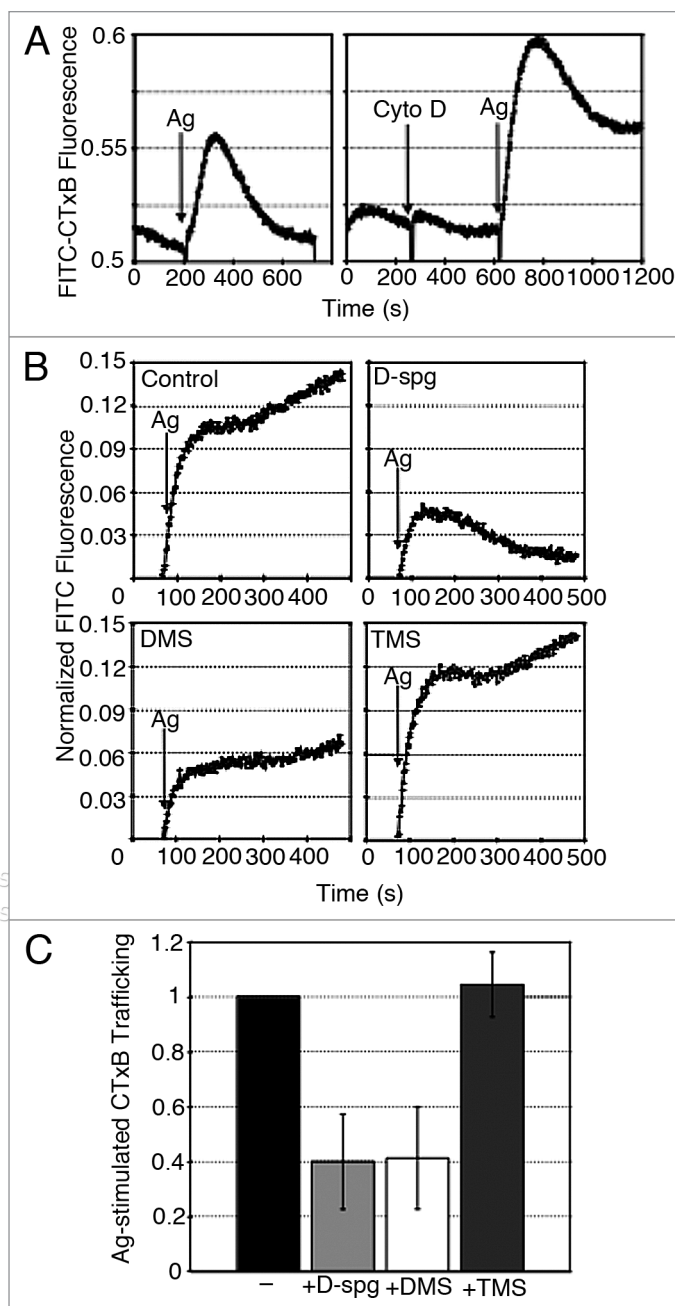


**Figure 2.** D-sphingosine and DMS, but not TMS, inhibit antigen-stimulated FITC-CTxB/GM<sub>1</sub> trafficking. (A) RBL cells exhibit outward trafficking of FITC-CTxB due to antigen (left) that is enhanced by cytochalasin D (Cyto D; right). (B) Representative time courses for stimulated trafficking in the presence or absence of sphingosine derivatives (8  $\mu$ M) as indicated. (C) Summary of the effects of sphingosines on trafficking responses integrated for 420 s. Data are averages from four independent experiments, +/-SD.

differences in the time courses of these attenuated responses. In contrast, TMS does not alter the magnitude or kinetics of the stimulated response. Figure 2C compares the integrated responses to Ag in the presence and absence of these sphingosine derivatives as averages of four independent experiments. As indicated, 8  $\mu$ M D-sphingosine or DMS both inhibit this integrated response by

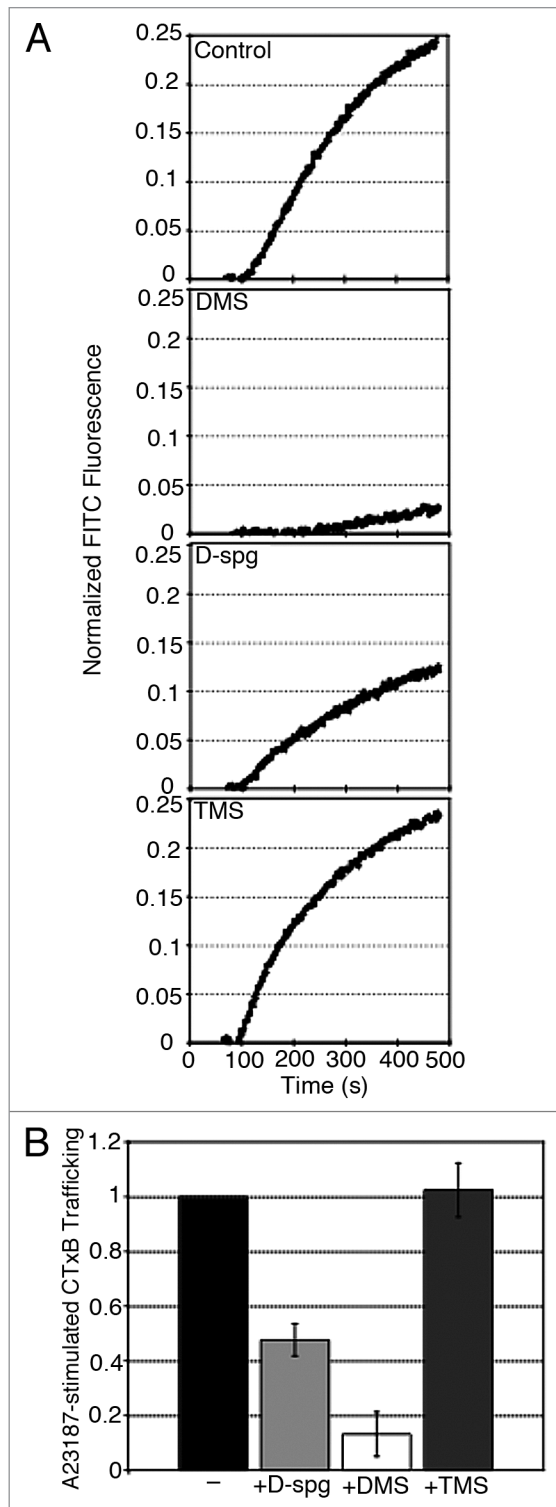


**Figure 3.** Sphingosine derivatives inhibit recycling endosome trafficking triggered by calcium ionophore. (A) Representative time courses showing that D-sphingosine and DMS, but not TMS, inhibit calcium ionophore-stimulated trafficking of FITC-CTxB/GM1. RBL cells were stimulated with 1  $\mu$ M A23187 in the presence or absence of 8  $\mu$ M sphingosine derivatives. (B) Summary of inhibitory effects averaging three independent experiments,  $\pm$ SD.

~60%. In other experiments, we found that lower concentrations of these derivatives inhibit to lesser extents: 4  $\mu$ M D-sphingosine causes less than half of the inhibition observed at 8  $\mu$ M (data not shown). At concentrations of these derivatives greater than 10  $\mu$ M, some cell lysis is variably detected, as indicated by progressive leakage of the  $\text{Ca}^{2+}$  indicator, indo-1 (data not shown). In subsequent experiments, we compared the effects of these sphingosine derivatives at the optimal dose of 8  $\mu$ M. In other experiments, we found that the stereoisomer of D-sphingosine, L-sphingosine, inhibits the outward trafficking of FITC-CTxB bound to GM<sub>1</sub> to a similar extent at similar concentrations (data not shown), suggesting that stereospecific binding to a target protein is unlikely to be the mechanism of inhibition.

We subsequently tested the effects of sphingosine derivatives on outward trafficking of FITC-CTxB/GM<sub>1</sub> stimulated by the  $\text{Ca}^{2+}$  ionophore A23187. A23187 is a mobile carrier of divalent cations that increases intracellular  $\text{Ca}^{2+}$  levels in the absence of inositol 1,4,5-trisphosphate ( $\text{IP}_3$ )-dependent antigen-stimulated  $\text{Ca}^{2+}$  release from intracellular stores, thereby allowing us to bypass early signaling steps. In initial experiments we found that stimulation with A23187 caused robust outward trafficking, even in the absence of cytochalasin D (Fig. 3A). Under these conditions, D-sphingosine and DMS substantially inhibit outward trafficking of FITC-CTxB bound to GM<sub>1</sub>, and DMS is somewhat more effective than D-sphingosine (Fig. 3A and B). The basis for this difference is unclear. Similarly, we found that D-sphingosine and DMS inhibit outward trafficking of FITC-CTxB stimulated by thapsigargin, which stimulates SOCE by inhibiting SERCA pumps in the endoplasmic reticulum (ER; data not shown). Together, these results indicate that sphingosine derivatives inhibit FITC-CTxB trafficking downstream from the earliest signaling events stimulated by Fc $\epsilon$ RI. In fact, no significant change in stimulated phosphorylation of Fc $\epsilon$ RI  $\beta$  and  $\gamma$  subunits is detected following addition of the sphingosine derivatives tested in this study (data not shown).

To evaluate whether outward trafficking of recycling endosomes occurs in adherent RBL mast cells, we developed an imaging method to detect this process. For these experiments, we first blocked GM<sub>1</sub> at the plasma membrane with unlabeled CTxB, then stimulated cells in the presence of excess Alexa488-CTxB and monitored its binding to newly-trafficked GM<sub>1</sub> at the plasma membrane using an imaging analysis method that we previously developed.<sup>28</sup> As shown in Figure 4A, A23187 stimulates a significant increase in the trafficking of GM<sub>1</sub> to the plasma membrane in adherent RBL cells. Furthermore, D-sphingosine inhibits this stimulated outward trafficking of GM<sub>1</sub> by ~60% under these conditions (Fig. 4B), consistent with results for stimulated trafficking of FITC-CTxB bound to GM<sub>1</sub> in suspended RBL cells (Fig. 3). Thus, GM<sub>1</sub> outward trafficking is stimulated in adherent RBL cells, indicating that this process is not restricted to suspended cells or to CTxB/GM<sub>1</sub> complexes. Furthermore, these results establish an alternative, single cell imaging assay for stimulated outward trafficking of recycling endosomes.

**Degranulation of secretory lysosomes is inhibited by sphingosine derivatives.** To determine whether sphingosines inhibit stimulated release of secretory lysosomes in these cells, we



carried out degranulation assays with suspended RBL-2H3 cells in the presence of cytochalasin D to match the conditions used in our FITC-CTxB recycling endosome trafficking experiment. As shown in **Figure 5**, both D-sphingosine and DMS inhibit degranulation responses similar to the extents as they inhibit FITC-CTxB outward trafficking. As in the previous trafficking experiments, TMS had little effect on the degranulation response, consistent with its incapacity to flip to the inner leaflet of the plasma membrane.

**Sphingosine derivatives inhibit  $\text{Ca}^{2+}$  mobilization in stimulated RBL mast cells.** Because DMS and D-sphingosine inhibit both RE trafficking and degranulation responses, it is likely that they inhibit a signaling step that is important for both. Although  $\text{Ca}^{2+}$  mobilization and protein kinase C (PKC) activation are important for secretory granule exocytosis in these cells,<sup>29,30</sup> inhibition of PKC has little effect on CTxB/GM<sub>1</sub> outward trafficking.<sup>2</sup>  $\text{Ca}^{2+}$  mobilization has two well-identified phases in RBL-mediated signaling: release from intracellular stores via IP<sub>3</sub> and IP<sub>3</sub> receptors on the ER followed by extracellular calcium influx through Orail.<sup>31</sup>

To evaluate whether sphingosine derivatives affect stimulated  $\text{Ca}^{2+}$  release from stores as well as influx, we stimulated RBL cells in the absence of extracellular  $\text{Ca}^{2+}$ , then replenished  $\text{Ca}^{2+}$  after several hundred seconds. In untreated cells, antigen addition causes a rapid increase in the intracellular  $\text{Ca}^{2+}$  concentration that returns to baseline following store depletion (**Fig. 6A**). When  $\text{Ca}^{2+}$  is added back into the extracellular buffer, stimulated  $\text{Ca}^{2+}$  influx results in a sustained increase in cytoplasmic  $\text{Ca}^{2+}$ . Addition of D-sphingosine or DMS to unstimulated cells causes small and/or transient increases in cytoplasmic  $\text{Ca}^{2+}$ , and subsequent addition of antigen results in reduced stimulated release from stores. In four separate experiments with 8  $\mu\text{M}$  D-sphingosine, antigen-stimulated  $\text{Ca}^{2+}$  release from stores was reduced by 85  $\pm$  19% (SD). Similar to trafficking and degranulation responses, treatment with TMS has negligible effects on antigen-induced calcium release from stores (**Fig. 5D**). Addition of  $\text{Ca}^{2+}$  subsequent to antigen for D-sphingosine and DMS-treated cells results in smaller responses than with antigen alone, whereas the antigen response in TMS-treated cells is identical to that of untreated cells (**Fig. 5A–D**). These results indicate that D-sphingosine and DMS inhibit both antigen-stimulated  $\text{Ca}^{2+}$  release from stores, as well as stimulated  $\text{Ca}^{2+}$  influx.

To quantify effects of sphingosine derivatives on  $\text{Ca}^{2+}$  responses in the presence of extracellular  $\text{Ca}^{2+}$ , we compared time-integrated  $\text{Ca}^{2+}$  responses to antigen. As summarized in **Figure 6E**, both D-sphingosine and DMS block much of the antigen-stimulated  $\text{Ca}^{2+}$  response when compared to either untreated cells or those treated with TMS. These results, together with others described above, make it likely that D-sphingosine and DMS inhibit degranulation and outward trafficking of

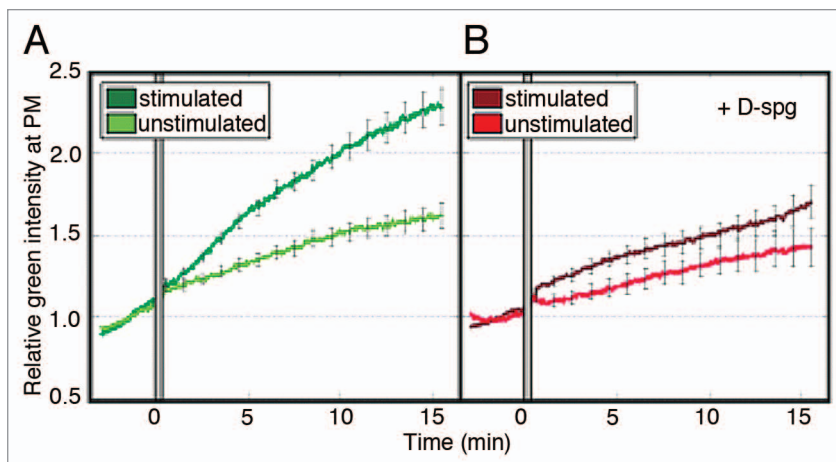


**Figure 4.** Live cell imaging of GM<sub>1</sub> trafficking to the plasma membrane in response to stimulation by calcium ionophore. Dynamics are monitored as mean plasma membrane fluorescence of Alexa488-CTxB in the absence (A) or presence (B) of 8  $\mu\text{M}$  D-sphingosine, normalized to each pre-stimulation average. Gray bars indicate time of A23187 addition. Each condition represents average data for 15–28 individual cells from 4–5 independent experiments. Error bars show SEM.

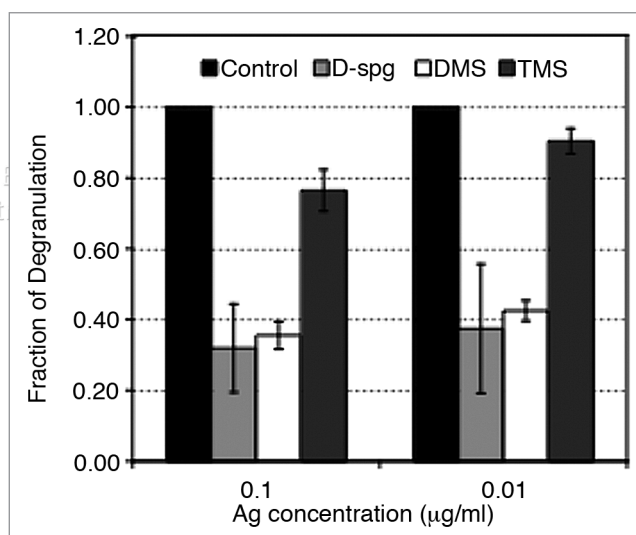


**Figure 5.** Degranulation responses in RBL-2H3 cells are similarly inhibited by D-sphingosine and DMS, but not TMS. Degranulation measured by  $\beta$ -hexosaminidase release following antigen stimulation at concentrations indicated in the presence of 2  $\mu\text{M}$  cytochalasin D  $\pm$  sphingosine derivatives, expressed as fraction of control (antigen-stimulated) cell degranulation. Average of 3 independent experiments,  $\pm$  SD.

recycling endosomes at least in part by inhibiting  $\text{Ca}^{2+}$  mobilization, which is important for these more downstream exocytotic processes. Consistent with this, we find that these derivatives similarly inhibit the sustained, influx phase of A23187-mediated  $\text{Ca}^{2+}$  mobilization and A23187-stimulated degranulation (data not shown). These results are accountable by the inhibition of store-operated  $\text{Ca}^{2+}$  entry by these long chain bases, as this process is activated by A23187, as well as by antigen and thapsigargin, and is important for stimulated degranulation in mast cells.<sup>23</sup>

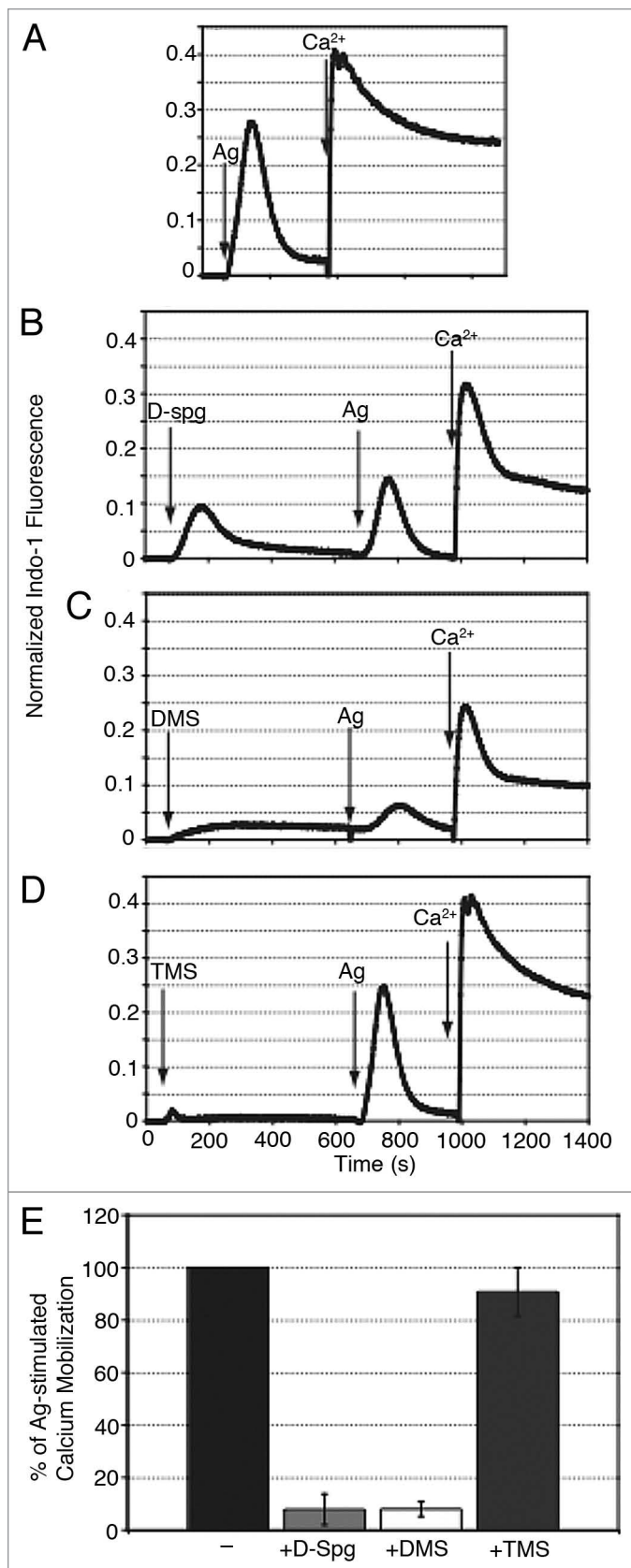


**Figure 6.** Sphingosine derivatives inhibit release from  $\text{Ca}^{2+}$  stores in addition to blocking  $\text{Ca}^{2+}$  influx. (A–D) RBL cells labeled with indo-1, then washed into  $\text{Ca}^{2+}$ -free buffer, were treated with sphingosine derivatives (8  $\mu\text{M}$ ), followed by antigen (0.8  $\mu\text{g}/\text{ml}$  DNP-BSA) and  $\text{Ca}^{2+}$  (2 mM) as indicated. Data are representative of 2–4 independent experiments. (E) Summary of indo-1-monitored time-integrated responses to antigen in the presence of extracellular  $\text{Ca}^{2+}$ , with or without 8  $\mu\text{M}$  sphingosine derivatives. Data are averages from 4–5 independent experiments,  $\pm$ SD.

D-sphingosine and DMS displace the polybasic MARCKS effector domain from interactions with polyphosphoinositides at the plasma membrane. To investigate the mechanism by which D-sphingosine and DMS inhibit  $\text{Ca}^{2+}$  mobilization and  $\text{Ca}^{2+}$ -dependent secretory processes, we utilized the polybasic myristoylated, alanine-rich PKC substrate effector domain (MARCKS ED), which is a 25 amino acid sequence containing 13 basic residues that binds tightly to the plasma membrane via interactions with acidic phospholipids.<sup>32</sup> Meyer and colleagues showed that this association with the inner leaflet of the plasma membrane is dependent on interactions with polyphosphoinositides.<sup>21</sup> Full-length MARCKS dissociates from the plasma membrane in response to PKC-mediated phosphorylation of three serine residues in the effector domain. We mutated these residues to alanines to prevent this dissociation and used this MARCKS ED<sup>SA3</sup> as an inhibitor of polyphosphoinositide accessibility.

As shown in Figure 7A, MARCKS ED<sup>SA3</sup>, tagged with a monomeric red fluorescent protein (mRFP), associates preferentially with the plasma membrane, with some additional label in the cytoplasm and nucleus to varying extents. Consistent with expectations, activation of PKC by 8 nM phorbol 12-myristate 13-acetate causes dissociation of mRFP-MARCKS ED from the plasma membrane but does not induce the dissociation of mRFP-MARCKS ED<sup>SA3</sup> (data not shown). To quantify the partitioning of mRFP-MARCKS ED<sup>SA3</sup> between the plasma membrane and the cytoplasm, we measured the intensity profile of a line across individual cells as illustrated in Figure 7A and described in Materials and Methods. In six separate experiments in which the ratio of plasma membrane to cytoplasmic intensity of mRFP-MARCKS ED<sup>SA3</sup> was quantified in at least 15 cells per sample for each experiment, the average value for this ratio in control cells is  $7.0 \pm 0.9$  (SEM).

To establish whether mRFP-MARCKS ED<sup>SA3</sup> could be displaced from the plasma membrane by perturbations known to alter polyphosphatidylinositide levels, we measured its plasma membrane to cytoplasmic fluorescence ratio to evaluate the effects of antigen stimulation and pharmacological inhibitors of polyphosphoinositide kinases (Fig. 7). Wortmannin is a potent inhibitor of phosphatidylinositol (PI) 3-kinases,<sup>33</sup> but at a concentration sufficient to completely inhibit this enzyme family (200 nM), wortmannin did not induce detectable dissociation of mRFP-MARCKS ED<sup>SA3</sup> from the plasma membrane (data not shown). At higher concentrations, wortmannin is an effective inhibitor of Type III PI4-kinases,<sup>34</sup> with  $\text{K}_i$ 's of  $\sim 100$  nM. As shown in Figure 7B, treatment of these cells with 10  $\mu\text{M}$  wortmannin for 10 min at  $37^\circ\text{C}$  reduced the association of mRFP-MARCKS ED<sup>SA3</sup> with the plasma membrane

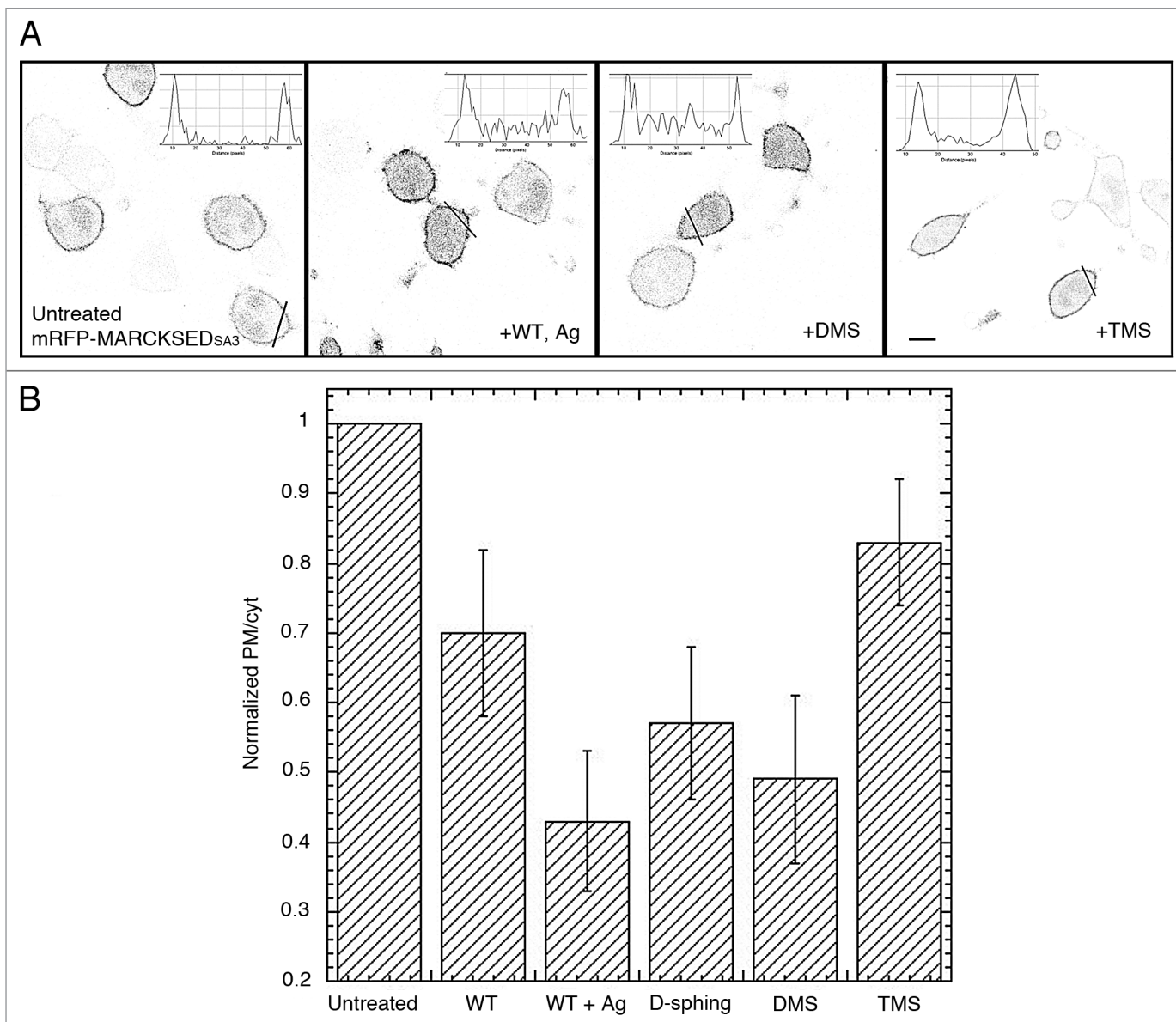


**Figure 7.** Dissociation of mRFP-MARCKS ED<sup>SA3</sup> from the plasma membrane due to various treatments. (A) Representative inverted confocal images showing mRFP-MARCKS ED<sup>SA3</sup>-expressing RBL cells in the absence (first (left)) or following treatment with 10  $\mu$ M wortmannin (WT) and 0.8  $\mu$ g/ml antigen (second), 8  $\mu$ M DMS (third), or 8  $\mu$ M TMS (fourth). Lines through cells in each panel illustrate sections chosen for line scan analysis, and profiles for these are shown as inserts in each panel. (B) Summary of effects of various treatments on the normalized ratio of mRFP-MARCKS ED<sup>SA3</sup> fluorescence at the plasma membrane to average cytoplasmic fluorescence determined as described in Materials and Methods. Data represents the average of 3–4 experiments per sample (>50 cells total per sample),  $\pm$ SD.

by ~30%, suggesting that PI4-P contributes to the binding of this probe to the plasma membrane.

Antigen stimulation of PI 4,5-bisphosphate (PIP<sub>2</sub>) hydrolysis is expected to reduce the effective concentration of PIP<sub>2</sub> at the plasma membrane and thereby reduce the binding of MARCKS ED.<sup>21,31</sup> However, antigen stimulation of RBL cells causes them to ruffle and flatten,<sup>35</sup> making it difficult to quantify mRFP-MARCKS ED<sup>SA3</sup> at the plasma membrane. Wortmannin prevents these morphological changes while permitting stimulated hydrolysis of PIP<sub>2</sub>, as evidenced by antigen-stimulated, IP<sub>3</sub>-dependent Ca<sup>2+</sup> mobilization under these conditions

(data not shown). As shown in **Figure 7B**, antigen stimulation in the presence of 10  $\mu$ M wortmannin further reduces the association of mRFP-MARCKS ED<sup>SA3</sup> at the plasma membrane compared to wortmannin alone, consistent with sensitivity of this association to PIP<sub>2</sub> hydrolysis.

We next determined whether sphingosine derivatives can displace mRFP-MARCKS ED<sup>SA3</sup> from the plasma membrane under conditions in which these long chain bases inhibit signaling. As shown in **Figure 7B**, addition of 8  $\mu$ M D-sphingosine for 10 min at 37°C causes substantial displacement of mRFP-MARCKS ED<sup>SA3</sup> from the plasma membrane, and DMS at



the same concentration causes a slightly larger displacement of ~50%, similar to that caused by 10  $\mu$ M wortmannin + antigen. In contrast, TMS causes a relatively small reduction (<20%) in the plasma membrane to cytoplasmic ratio of mRFP-MARCKS ED<sup>SA3</sup>. This effect may be due in part to impurities in the TMS preparation that can flip to the inner leaflet or, alternatively, to an increased plasma membrane surface area that is induced when TMS partitions into the outer leaflet (Fig. 1).

Taken together, these results provide evidence that sphingosine derivatives that flip from the outer to the inner leaflet of the plasma membrane substantially reduce the binding of mRFP-MARCKS ED<sup>SA3</sup> to the plasma membrane. Because of the electrostatic basis for this association, it is likely that the positively charged headgroups of D-sphingosine and DMS provide electrostatic neutralization of polyphosphoinositides at the inner leaflet of the plasma membrane, thus competing with mRFP-MARCKS ED<sup>SA3</sup> for binding to these negatively charged phospholipids.

## Discussion

The plasma membrane is a dynamic organelle, with continuous turnover of lipids and proteins mediated by membrane trafficking and other processes. Recycling endosomes, also known as the endosomal recycling compartment, provide a pool of readily available membrane components that can be trafficked to the cell surface under resting and stimulatory conditions.<sup>2,36</sup> The small GTPases Rab11 and Arf6 have been identified as regulators of recycling endosomes.<sup>37-39</sup> Mutation of Rab11 to an inactive GTPase inhibits trafficking of transferrin-containing recycling endosomes,<sup>40</sup> whereas an analogous mutation in Arf6 inhibits trafficking of GM<sub>1</sub>, but not transferrin receptors, from recycling endosomes to the plasma membrane, suggesting that at least two distinct subsets of recycling endosomes participate in these processes.<sup>41</sup>

Although much is now known about the proteins and signaling pathways that regulate trafficking of recycling endosomes, the roles of this trafficking in cell physiology are poorly understood in most cell types. To begin to investigate these roles in mast cells, we characterized the effects of sphingosine derivatives on antigen-stimulated outward trafficking of FITC-CTxB-labeled recycling endosomes. We found that D-sphingosine and DMS are similarly effective inhibitors of this process, and this inhibition correlates with their capacity to flip from the outer leaflet of the plasma membrane to its inner leaflet, as monitored by both transient relief of FITC-CTxB self-quenching at the plasma membrane, and by a time-dependent increase in cytoplasmic pH. In contrast to these sphingosines, most TMS remains in the outer leaflet of the plasma membrane, as monitored by a more sustained increase in FITC-CTxB fluorescence and a smaller, more slowly developing increase in cytoplasmic pH (Fig. 1). Consistent with these differences, TMS does not inhibit stimulated outward trafficking of FITC-CTxB-labeled recycling endosomes (Figs. 2 and 3). Similarly, D-sphingosine and DMS inhibit antigen-stimulated degranulation responses by ~60% under these conditions, whereas TMS inhibits this response to a much smaller extent (Fig. 5). Recently, D-sphingosine has been shown

to inhibit exocytotic release of insulin and Glut4 expression at the plasma membrane of beta cells, and a similar electrostatic mechanism of inhibition has been implicated.<sup>42</sup>

Similar trends are observed for the effects of these derivatives on antigen-stimulated Ca<sup>2+</sup> responses. These results are consistent with a previous study that demonstrated inhibition of IP<sub>3</sub>- and thapsigargin-stimulated Ca<sup>2+</sup> release-activated Ca<sup>2+</sup> (CRAC) channels by D-sphingosine and DMS.<sup>24</sup> In a more recent study, we showed that these derivatives inhibit store-operated Ca<sup>2+</sup> entry by interfering with the coupling between the CRAC channel, Orai1, and the ER Ca<sup>2+</sup> sensor protein, STIM1.<sup>20</sup> However, we now find that these sphingosine derivatives inhibit antigen-stimulated Ca<sup>2+</sup> release from ER stores, indicating an additional effect on antigen-stimulated Ca<sup>2+</sup> responses at a step that precedes store-operated Ca<sup>2+</sup> entry (Fig. 6). Similar to results for stimulated outward trafficking of recycling endosomes and degranulation, we find that TMS fails to inhibit both antigen-stimulated Ca<sup>2+</sup> release from stores and Ca<sup>2+</sup> influx, suggesting that the redistribution of D-sphingosine and DMS to the inner leaflet of the plasma membrane are important for their inhibitory effects.

In some previous studies, inhibition of Ca<sup>2+</sup> mobilization and other signaling processes by DMS was suggested to be due to inhibition of the production of sphingosine-1-phosphate by sphingosine kinases.<sup>43,44</sup> From our present results and those of Mathes et al.,<sup>24</sup> this explanation seems unlikely, as both DMS and the substrate for sphingosine-1-kinase, D-sphingosine, similarly inhibit Ca<sup>2+</sup> mobilization and exocytosis of both recycling endosomes and secretory lysosomes. Although more complex mechanisms, such as substrate inhibition of sphingosine 1-kinase, cannot be excluded,<sup>45</sup> the simplest explanation for our results is that sphingosine derivatives inhibit antigen-stimulated signaling processes by a different mechanism than interference with sphingosine 1-phosphate production. In this regard, Olivera et al. showed that knockout of sphingosine kinase 2, which inhibits Ca<sup>2+</sup> mobilization in mast cells, significantly increases intracellular levels of D-sphingosine.<sup>46</sup> Thus, we suggest that alterations in endogenous levels of D-sphingosine may directly modulate Ca<sup>2+</sup> and other signaling processes.

One mechanism by which basic lipids such as sphingosines might alter signaling pathways is electrostatic neutralization of acidic lipids. These lipids, including polyphosphatidylinositides, are preferentially localized at the inner leaflet of the plasma membrane, and they serve multiple roles in cell signaling.<sup>47</sup> PIP<sub>2</sub>, for example, serves as a substrate for phospholipase C-mediated production of IP<sub>3</sub> in the initiation of store-operated Ca<sup>2+</sup> entry,<sup>48</sup> and it has also been implicated in exocytotic processes via plasma membrane targeting of Ca<sup>2+</sup>-sensing proteins such as synaptotagmins.<sup>49</sup> As described above, Meyer and colleagues investigated the roles of polyphosphoinositides in plasma membrane targeting of various signaling proteins, and they showed that the strong association of the polybasic effector domain of the PKC substrate MARCKS with the plasma membrane is largely due to electrostatic interactions with polyphosphoinositides.<sup>21</sup> We took advantage of these observations to test whether sphingosines can compete for electrostatic interactions between polyphosphoinositides at the plasma membrane and mRFP-MARCKS



ED that is mutated to prevent its PKC-mediated dissociation. We found that both D-sphingosine and DMS substantially reduce the plasma membrane-to-cytoplasmic ratio of mRFP-MARCKS ED<sup>SA3</sup>, whereas TMS causes a smaller decrease in this ratio (Fig. 7).

Interestingly, wortmannin at a concentration that effectively inhibits PI3-kinases (200 nM) does not significantly reduce association of mRFP-MARCKS ED<sup>SA3</sup>, whereas 10  $\mu$ M wortmannin, which inhibits PI4-P synthesis,<sup>34</sup> causes substantial dissociation that is enhanced by antigen, most likely due to stimulated PIP<sub>2</sub> hydrolysis (Fig. 7B). These results suggest that PI4-P contributes to the electrostatic association of mRFP-MARCKS ED<sup>SA3</sup> with the plasma membrane, in addition to the contribution of PIP<sub>2</sub>. The similar extent of mRFP-MARCKS ED<sup>SA3</sup> dissociation caused by D-sphingosine and DMS compared to that caused by 10  $\mu$ M wortmannin and antigen suggests that these sphingosine derivatives effectively compete with mRFP-MARCKS ED<sup>SA3</sup> for binding to PIP<sub>2</sub> and PI4-P at the plasma membrane.

These results, taken together, indicate that D-sphingosine and DMS are effective inhibitors of Fc $\epsilon$ RI-mediated signaling because of their capacity to compete electrostatically with proteins for binding to polyphosphoinositides at the inner leaflet of the plasma membrane. However, we cannot exclude roles for electrostatic neutralization of other classes of negatively charged phospholipids by these sphingosine derivatives for their inhibitory effects on Ca<sup>2+</sup> mobilization leading to stimulated exocytosis of recycling endosomes and secretory lysosomes. Further studies will be necessary to assess more directly the phospholipid specificity of these inhibitory effects. Nonetheless, our results show that electrostatic neutralization of negatively charged phospholipids, including polyphosphoinositides, is likely to be relevant to a large number of studies in which sphingosine derivatives have been shown to be effective inhibitors of cell signaling.

## Materials and Methods

**Reagents.** FITC-cholera toxin B subunit (FITC-CTxB), D-sphingosine, cytochalasin D, 4-methylumbelliferyl-N-acetyl- $\beta$ -D-glucosaminide, and nigericin were obtained from Sigma-Aldrich Chem., Co., (Saint Louis, MO). BCECF-AM, indo-1 AM, and Alexa488-CTxB were purchased from Invitrogen Corp., (Carlsbad, CA). A23187 was from EMD (San Diego, CA). N,N'-dimethylsphingosine and N,N',N''-trimethylsphingosine were purchased from Avanti Polar Lipids (Alabaster, AL). Mouse monoclonal anti-dinitrophenyl (DNP) IgE was purified as previously described.<sup>14</sup> Multivalent antigen, DNP-BSA, contained an average of 15 DNP groups as previously described.<sup>2</sup>

**Cell culture.** RBL-2H3 mast cells were cultured in minimum essential media with 20% fetal bovine serum (Atlanta Biologicals) and 10  $\mu$ g/ml gentamicin sulfate (RBL Media) as described previously.<sup>15</sup> All tissue culture reagents were obtained from Invitrogen unless otherwise noted. For antigen stimulation, cells were sensitized with 2–5 fold molar excess of anti-DNP IgE for 2–24 hr prior to experiments. Confluent cells were harvested with 135 mM NaCl, 5 mM KCl, 20 mM Hepes, 1.5 mM EDTA,

pH 7.4, and resuspended in either buffered saline solution (BSS: 135 mM NaCl, 5 mM KCl, 1.8 mM CaCl<sub>2</sub>, 1 mM MgCl<sub>2</sub>, 5.6 mM glucose, 1 mg/ml BSA and 20 mM HEPES, pH 7.4) or RBL media with 20 mM HEPES.

**Cholera toxin B trafficking.** For steady state spectrofluorimeter experiments, RBL-2H3 cells were harvested and resuspended at 4  $\times$  10<sup>6</sup> cells/ml in RBL media with 20 mM Hepes. FITC-CTxB was added to a final concentration of 3  $\mu$ g/ml and incubated at 37°C for 2 hours. Cells were washed 2 times and resuspended at a final concentration of 2  $\times$  10<sup>6</sup> cells/ml in BBS, stirred continuously in an acrylic cuvette and maintained at a temperature of 37°C. Fluorescence measurements were made with an SLM 8000C fluorescence spectrophotometer as previously described.<sup>2</sup> Following additions as indicated in figure legends, cells were stimulated with either 4  $\mu$ g/ml DNP-BSA in the presence or absence of 2  $\mu$ M cytochalasin D or with 1  $\mu$ M calcium ionophore A23187, and changes in FITC fluorescence were monitored.

For analysis, Excel (Microsoft) software was used. Briefly, using recorded pre-stimulation data, the TREND function was used to generate a linear baseline prediction that extended over the stimulation time course. This baseline was then subtracted from the stimulated data and the resulting data were normalized for variations in initial fluorescence.

**Degranulation.** IgE-sensitized RBL-2H3 cells were harvested and resuspended in BSS at 2  $\times$  10<sup>6</sup> cells/ml with 2  $\mu$ M cytochalasin D. Cells were incubated with sphingosine derivatives for 5 minutes prior to stimulation. Stimulated cells were incubated in a water bath with shaking at 37°C for 1 hr, then placed on ice for 10 minutes, and centrifuged for 5 minutes at 900 rpm at 4°C as previously described.<sup>16</sup> Following centrifugation, 25  $\mu$ l cell supernatants were plated in triplicate in black flat bottomed 96 well plates (Costar) with 100  $\mu$ l substrate solution (1.2 mM 4-methylumbelliferyl-N-acetyl- $\beta$ -D-glucosaminide in acetate buffer (0.12 M acetic acid, pH 4.4) and processed for measurement of  $\beta$ -hexosaminidase activity as previously described.<sup>17</sup>

**Measurement of intracellular pH.** RBL cells were harvested and resuspended in BSS at 1  $\times$  10<sup>7</sup> cells/ml and equilibrated to 37°C. BCECF-AM (3.3.  $\mu$ g/ml) was loaded into cells by incubating for 1–1.5 min, then diluting to 2  $\times$  10<sup>6</sup> cells/ml and rotating slowly for 30 min at 37°C. Washed cells were used at a final concentration of 1  $\times$  10<sup>6</sup> cells/ml, and fluorescence was measured using SLM 8000C fluorescence spectrophotometer, with excitation at 490 nm and emission at 510 nm. Changes in pH were determined using a calibration curve generated by dilution of cells into calibration buffer at pH values of 6, 6.5, 7, 7.5 and 8 in the presence of 10  $\mu$ M nigericin.<sup>18</sup>

**Measurement of intracellular Ca<sup>2+</sup>.** Stimulated Ca<sup>2+</sup> responses were monitored as described previously.<sup>15</sup> Briefly, RBL cells were loaded with the calcium indicator indo-1 AM, washed, and calcium mobilization in response to stimulation was measured using SLM 8000C fluorescence spectrophotometer. Time-integrated responses were determined as the area under the stimulated time-course minus the baseline over 400 s, normalized to the maximal response in Triton X-100 lysed cells.<sup>19</sup>

**Confocal fluorescence microscopy.** Cells were labeled with Alexa488-CTxB as described for FITC-CTxB above, incubated

with or without sphingosine derivatives in BSS for 10 min at 37°C, then fixed in 4% paraformaldehyde for 15 min at room temperature. Fixed cells were imaged with a BioRad MRC 600 confocal system and a Zeiss Axiovert 10 microscope and x100 objective.

For detection of interactions between sphingosine derivatives and polyphosphoinositides at the plasma membrane, mRFP-MARCKS ED<sup>SA3</sup> was expressed in RBL cells by transient transfection with Eugene HD (Roche Diagnostics, Indianapolis, IN) as previously described.<sup>20</sup> mRFP-MARCKS ED<sup>SA3</sup> was made from YFP-MARCKS ED<sup>21</sup> by exchanging YFP for mRFP by using the Nhe I and Hind III restriction sites. Subsequently, the QuikChange Site-Directed Mutagenesis Kit (Stratagene) was used to insert successive mutations of serines 159, 163 and 170 (full length MARCKS notation) to alanines. Changes were confirmed by DNA sequence analysis. For these experiments, transfected cells in MatTek 35 mm culture dishes (MatTek Corp., Ashland, MA) were treated with sphingosine derivatives or other agents as described in Results, then fixed and imaged as above using a x63 achromatically corrected objective (NA 1.4). Line scan analysis of equatorial confocal sections with Image J (NIH) was used to determine the ratio of plasma membrane to cytoplasmic localization for mRFP-MARCKS ED<sup>SA3</sup> after various treatments. Ratios determined for each sample are averages of 15–20 cells in 4–5 images.

To monitor GM<sub>1</sub> trafficking to the plasma membrane by quantitative confocal imaging, RBL cells in MatTek culture

dishes were first incubated with 5 µg/ml unlabeled CTxB and 2 µg/ml DiI-C16 (Molecular Probes/Invitrogen) for 5 min at 25°C to block plasma membrane-associated GM<sub>1</sub> and to label the plasma membrane. Cells washed in BSS were then imaged in the presence of 1 µg/ml Alexa488-CTxB and 2 µM cytochalasin D, with or without 8 µM D-sphingosine, and stimulated by 4.8 µM A23187 at 25°C to minimize label exchange and internalization. Confocal images were acquired using a Leica TCS SP2 upright microscope system (Leica Microsystems, Exton, PA) with a x63, 0.9 NA HCX APO LU-V-I water immersion objective. Green and red images were collected sequentially to minimize bleed-through, with a rate of 3 s/frame. For Alexa488-CTxB,  $\lambda_{ex}$  = 488,  $\lambda_{em}$  = 500–550; for DiI-C16,  $\lambda_{ex}$  = 543,  $\lambda_{em}$  = 560–630. Image analysis was carried out as previously described.<sup>28</sup> This method uses the plasma membrane-localized DiI-C16 label to create a binary plasma membrane mask that is used to define the Alexa488 fluorescence of interest. The average intensity of Alexa488-CTxB fluorescence in this region is calculated for each frame and plotted as a function of time.

# Acknowledgements

We thank Dr. Tobias Meyer (Stanford University) for the YFP-MARCKS ED construct and Ms. Carol Bayles for maintaining the Cornell Microscopy and Imaging Facility. This work was supported by NIH Grant R01 AI022449.

# References

- Gilfillan AM, Rivera J. The tyrosine kinase network regulating mast cell activation. *Immunol Rev* 2009; 228:149-69.
- Naal RM, Holowka EP, Baird B, Holowka D. Antigen-stimulated trafficking from the recycling compartment to the plasma membrane in RBL mast cells. *Traffic* 2003; 4:190-200.
- Taylor CW, Broad LM. Pharmacological analysis of intracellular Ca<sup>2+</sup> signalling: problems and pitfalls. *Trends Pharmacol Sci* 1998; 19:370-5.
- Hopkins CR, Trowbridge IS. Internalization and processing of transferrin and the transferrin receptor in human carcinoma A431 cells. *J Cell Biol* 1983; 97:508-21.
- Yamashiro DJ, Tycko B, Fluss SR, Maxfield FR. Segregation of transferrin to a mildly acidic (pH 6.5) para-Golgi compartment in the recycling pathway. *Cell* 1984; 37:789-800.
- Prigozhina NL, Waterman-Storer CM. Decreased polarity and increased random motility in PtK1 epithelial cells correlate with inhibition of endosomal recycling. *J Cell Sci* 2006; 119:3571-82.
- Ang AL, Taguchi T, Francis S, Folsch H, Murrells LJ, Pypaert M, et al. Recycling endosomes can serve as intermediates during transport from the Golgi to the plasma membrane of MDCK cells. *J Cell Biol* 2004; 167:531-43.
- Cresawn KO, Potter BA, Oztan A, Guerriero CJ, Ihrke G, Goldenring JR, et al. Differential involvement of endocytic compartments in the biosynthetic traffic of apical proteins. *EMBO J* 2007; 26:3737-48.
- Murray RZ, Kay JG, Sangermani DG, Stow JL. A role for the phagosome in cytokine secretion. *Science* 2005; 310:1492-5.
- Dyer N, Rebollo E, Dominguez P, Elkhatab N, Chavrier P, Daviet L, et al. Spermatocyte cytokinesis requires rapid membrane addition mediated by ARF6 on central spindle recycling endosomes. *Development* 2007; 134:4437-47.
- Varthakavi V, Smith RM, Martin KL, Derdowski A, Lapierre LA, Goldenring JR, et al. The pericentriolar recycling endosome plays a key role in Vpu-mediated enhancement of HIV-1 particle release. *Traffic* 2006; 7:298-307.
- Zhang M, Haapasalo A, Kim DY, Ingano LA, Pettingell WH, Kovacs DM. Presenilin/gamma-secretase activity regulates protein clearance from the endocytic recycling compartment. *Faseb J* 2006; 20:1176-8.
- Stow JL, Ching Low P, Offenhausser C, Sangermani D. Cytokine secretion in macrophages and other cells: Pathways and mediators. *Immunobiology* 2009; 214:601-12.
- Posner RG, Lee B, Conrad DH, Holowka D, Baird B, Goldstein B. Aggregation of IgE-receptor complexes on rat basophilic leukemia cells does not change the intrinsic affinity but can alter the kinetics of the ligand-IgE interaction. *Biochemistry* 1992; 31:5350-6.
- Gidwani A, Brown HA, Holowka D, Baird B. Disruption of lipid order by short-chain ceramides correlates with inhibition of phospholipase D and downstream signaling by FcεpsilonRI. *J Cell Sci* 2003; 116:3177-87.
- Mohr FC, Fewtrell C. The relative contributions of extracellular and intracellular calcium to secretion from tumor mast cells. Multiple effects of the proton ionophore carbonyl cyanide m-chlorophenylhydrazone. *J Biol Chem* 1987; 262:10638-43.
- Naal RM, Tabb J, Holowka D, Baird B. In situ measurement of degranulation as a biosensor based on RBL-2H3 mast cells. *Biosens Bioelectron* 2004; 20:791-6.
- Kamp F, Guo W, Souto R, Pilch PF, Corkey BE, Hamilton JA. Rapid flip-flop of oleic acid across the plasma membrane of adipocytes. *J Biol Chem* 2003; 278:7988-95.
- Field KA, Apgar JR, Hong-Geller E, Siraganian RP, Baird B, Holowka D. Mutant RBL mast cells defective in FcεpsilonRI signaling and lipid raft biosynthesis are reconstituted by activated Rho-family GTPases. *Mol Biol Cell* 2000; 11:3661-73.
- Calloway N, Vig M, Kinet JP, Holowka D, Baird B. Molecular clustering of STIM1 with Orai1/CRACM1 at the plasma membrane depends dynamically on depletion of Ca<sup>2+</sup> stores and on electrostatic interactions. *Mol Biol Cell* 2009; 20:389-99.
- Heo WD, Inoue T, Park WS, Kim ML, Park BO, Wandless TJ, et al. PI(3,4,5)P3 and PI(4,5)P2 lipids target proteins with polybasic clusters to the plasma membrane. *Science* 2006; 314:1458-61.
- Hewavitharana T, Deng X, Soboloff J, Gill DL. Role of STIM and Orai proteins in the store-operated calcium signaling pathway. *Cell Calcium* 2007; 42:173-82.
- Vig M, DeHaven WI, Bird GS, Billingsley JM, Wang H, Rao PE, et al. Defective mast cell effector functions in mice lacking the CRACM1 pore subunit of store-operated calcium release-activated calcium channels. *Nat Immunol* 2008; 9:89-96.
- Mathes C, Fleig A, Penner R. Calcium release-activated calcium current (ICRAC) is a direct target for sphingosine. *J Biol Chem* 1998; 273:25020-30.
- Bottega R, Epand RM, Ball EH. Inhibition of protein kinase C by sphingosine correlates with the presence of positive charge. *Biochem Biophys Res Commun* 1989; 164:102-7.
- Lau B, Macdonald PM. Determination of the pKa of membrane-bound N,N-dimethylsphingosine using deuterium NMR spectroscopy. *Biochim Biophys Acta* 1995; 1237:37-42.
- Devaux PF. Static and dynamic lipid asymmetry in cell membranes. *Biochemistry* 1991; 30:1163-73.
- Das R, Hammond S, Holowka D, Baird B. Real-time cross-correlation image analysis of early events in IgE receptor signaling. *Biophys J* 2008; 94:4996-5008.
- Wolfe PC, Chang EY, Rivera J, Fewtrell C. Differential effects of the protein kinase C activator phorbol 12-myristate 13-acetate on calcium responses and secretion in adherent and suspended RBL-2H3 mucosal mast cells. *J Biol Chem* 1996; 271:6658-65.

30. Taurog JD, Mendoza GR, Hook WA, Siraganian RP, Metzger H. Noncytotoxic IgE-mediated release of histamine and serotonin from murine mastocytoma cells. *J Immunol* 1977; 119:1757-61.
31. Ma HT, Beaven MA. Regulation of  $Ca^{2+}$  signaling with particular focus on mast cells. *Crit Rev Immunol* 2009; 29:155-86.
32. McLaughlin S, Aderem A. The myristoyl-electrostatic switch: a modulator of reversible protein-membrane interactions. *Trends in Biochem. Sci* 1995; 20:272-6.
33. Yano H, Nakanishi S, Kimura K, Hanai N, Saitoh Y, Fukui Y, et al. Inhibition of histamine secretion by wortmannin through the blockade of phosphatidylinositol 3-kinase in RBL-2H3 cells. *J Biol Chem* 1993; 268:25846-56.
34. Balla A, Balla T. Phosphatidylinositol 4-kinases: old enzymes with emerging functions. *Trends Cell Biol* 2006; 16:351-61.
35. Pfeiffer JR, Seagrave JC, Davis BH, Deanin GG, Oliver JM. Membrane and cytoskeletal changes associated with IgE-mediated serotonin release from rat basophilic leukemia cells. *J Cell Biol* 1985; 101:2145-55.
36. Maxfield FR, McGraw TE. Endocytic recycling. *Nat Rev Mol Cell Biol* 2004; 5:121-32.
37. D'Souza-Schorey C, van Donselaar E, Hsu VW, Yang C, Stahl PD, Peters PJ. ARF6 targets recycling vesicles to the plasma membrane: insights from an ultrastructural investigation. *J Cell Biol* 1998; 140:603-16.
38. Green EG, Ramm E, Riley NM, Spiro DJ, Goldenring JR, Wessling-Resnick M. Rab11 is associated with transferrin-containing recycling compartments in K562 cells. *Biochem Biophys Res Commun* 1997; 239:612-6.
39. Sonnichsen B, De Renzis S, Nielsen E, Rietdorf J, Zerial M. Distinct membrane domains on endosomes in the recycling pathway visualized by multicolor imaging of Rab4, Rab5 and Rab11. *J Cell Biol* 2000; 149:901-14.
40. Ren M, Xu G, Zeng J, De Lemos-Chiarandini C, Adesnik M, Sabatini DD. Hydrolysis of GTP on rab11 is required for the direct delivery of transferrin from the pericentriolar recycling compartment to the cell surface but not from sorting endosomes. *Proc Natl Acad Sci USA* 1998; 95:6187-92.
41. Balasubramanian N, Scott DW, Castle JD, Casanova JE, Schwartz MA. Arf6 and microtubules in adhesion-dependent trafficking of lipid rafts. *Nat Cell Biol* 2007; 9:1381-91.
42. Williams D, Vicogne J, Zaitseva I, McLaughlin S, Pessin JE. Evidence that electrostatic interactions between vesicle-associated membrane protein 2 and acidic phospholipids may modulate the fusion of transport vesicles with the plasma membrane. *Mol Biol Cell* 2009; 20:4910-9.
43. Jolly PS, Bektas M, Olivera A, Gonzalez-Espinosa C, Proia RL, Rivera J, et al. Transactivation of sphingosine-1-phosphate receptors by FcepsilonRI triggering is required for normal mast cell degranulation and chemotaxis. *J Exp Med* 2004; 199:959-70.
44. Itagaki K, Hauser CJ. Sphingosine 1-phosphate, a diffusible calcium influx factor mediating store-operated calcium entry. *J Biol Chem* 2003; 278:27540-7.
45. Prieschl EE, Csonga R, Novotny V, Kikuchi GE, Baumruker T. The balance between sphingosine and sphingosine-1-phosphate is decisive for mast cell activation after Fcε receptor I triggering. *J Exp Med* 1999; 190:1-8.
46. Olivera A, Mizugishi K, Tikhonova A, Ciaccia L, Odom S, Proia RL, Rivera J. The sphingosine kinase-sphingosine-1-phosphate axis is a determinant of mast cell function and anaphylaxis. *Immunity* 2007; 26:287-97.
47. Di Paolo G, De Camilli P. Phosphoinositides in cell regulation and membrane dynamics. *Nature* 2006; 443:651-7.
48. Rhee SG. Regulation of phosphoinositide-specific phospholipase C. *Annu Rev Biochem* 2001; 70:281-312.
49. Paddock BE, Striegel AR, Hui E, Chapman ER, Reist NE.  $Ca^{2+}$ -dependent, phospholipid-binding residues of synaptotagmin are critical for excitation-secretion coupling in vivo. *J Neurosci* 2008; 28:7458-66.

©2010 Landes Bioscience.  
Do not distribute.